



Tunnel diode oscillator measurements of the upper critical magnetic field of $\text{FeTe}_{0.5}\text{Se}_{0.5}$

Alain Audouard, Loïc Drigo, Fabienne Duc, Xavier Fabrèges, Ludovic Bosseaux, Pierre Toulemonde

► To cite this version:

Alain Audouard, Loïc Drigo, Fabienne Duc, Xavier Fabrèges, Ludovic Bosseaux, et al.. Tunnel diode oscillator measurements of the upper critical magnetic field of $\text{FeTe}_{0.5}\text{Se}_{0.5}$. *Journal of Physics: Condensed Matter*, 2014, 26 (18), pp.185701. 10.1088/0953-8984/26/18/185701 . hal-00955556

HAL Id: hal-00955556

<https://hal.science/hal-00955556>

Submitted on 4 Mar 2014

HAL is a multi-disciplinary open access archive for the deposit and dissemination of scientific research documents, whether they are published or not. The documents may come from teaching and research institutions in France or abroad, or from public or private research centers.

L'archive ouverte pluridisciplinaire **HAL**, est destinée au dépôt et à la diffusion de documents scientifiques de niveau recherche, publiés ou non, émanant des établissements d'enseignement et de recherche français ou étrangers, des laboratoires publics ou privés.

Tunnel diode oscillator measurements of the upper critical magnetic field of $\text{FeTe}_{0.5}\text{Se}_{0.5}$

Alain Audouard,^{*} Loïc Drigo,[†] Fabienne Duc,[‡] Xavier Fabrèges,[§] and Ludovic Bosseaux
*Laboratoire National des Champs Magnétiques Intenses (UPR 3228 CNRS,
INSA, UJF, UPS) 143 avenue de Rangueil, F-31400 Toulouse, France*

Pierre Toulemonde
*Univ. Grenoble Alpes, Institut NÉEL, F-38042 Grenoble, France.
CNRS, Institut NÉEL, F-38042 Grenoble, France.*
(Dated: March 4, 2014)

Temperature dependence of the upper critical magnetic field (H_{c2}) of single crystalline $\text{FeTe}_{0.5}\text{Se}_{0.5}$ ($T_c = 14.5$ K) have been determined by tunnel diode oscillator-based measurements in magnetic fields of up to 55 T and temperatures down to 1.6 K. The Werthamer-Helfand-Hohenberg model accounts for the data for magnetic field applied both parallel ($\mathbf{H} \parallel ab$) and perpendicular ($\mathbf{H} \parallel c$) to the iron conducting plane, in line with a single band superconductivity. Whereas Pauli pair breaking is negligible for $\mathbf{H} \parallel c$, Pauli contribution is evidenced for $\mathbf{H} \parallel ab$ with Maki parameter $\alpha = 1.4$, corresponding to Pauli field $H_P = 79$ T. As a result, the H_{c2} anisotropy ($\gamma = H_{c2}^{ab}/H_{c2}^c$) which is already rather small at T_c ($\gamma = 1.6$) further decreases as the temperature decreases and becomes smaller than 1 at liquid helium temperatures.

I. INTRODUCTION

The discovery of superconductivity in $\text{La}(\text{O}_{1-x}\text{F}_x)\text{FeAs}$ with T_c as high as 26 K¹ and, few months later, in $\text{Sm}(\text{O}_{1-x}\text{F}_x)\text{FeAs}$ with $T_c = 55$ K² (both of them illustrating the '1111' pnictide family) raised a tremendous interest for iron-based superconductors, notably in connection with the study of the interplay between superconductivity and magnetism (for recent reviews, see *e.g.*³⁻⁵). In that respect, determination of the temperature dependence of the upper critical magnetic field (H_{c2}) and its anisotropy yields information on the pair breaking mechanism and allows to decide between single and multigap superconductivity. Regarding the superconducting gap topology, the issue remains under debate since, for example, a nodeless two-gap picture is in agreement with the ARPES data of $\text{Ba}_{0.6}\text{K}_{0.4}\text{Fe}_2\text{As}_2$ ^{6,7} whereas nodal gaps have been inferred for $\text{BaFe}_2(\text{As}_{1-x}\text{P}_x)_2$ ^{8,9}, these two compounds belonging to the same '122' pnictide family.

Even though large magnetic fields are required to explore the low temperature part of the phase diagrams due to H_{c2} values as high as several tens of a Tesla, numerous works have been devoted to this issue. Reported data share a common feature, namely the decrease of the H_{c2} anisotropy as the temperature decreases, which nevertheless still requires a clear understanding. Oppositely, puzzling results regarding the temperature dependence of H_{c2} can be found in the literature. Indeed, in several cases, (i) the temperature dependence of H_{c2} exhibit a negative curvature consistent with the Werthamer-Helfand-Hohenberg (WHH) model, eventually including a Pauli contribution, for both \mathbf{H} parallel and perpendicular to the conducting ab plane ($\mathbf{H} \parallel ab$ and $\mathbf{H} \parallel c$, respectively). However, in several other cases, (ii) although the WHH model accounts for the data for $\mathbf{H} \parallel ab$, either a two-gap behaviour or a roughly lin-

ear temperature dependence is observed for $\mathbf{H} \parallel c$. In this latter case, even though multiple gap superconductivity is in agreement with ARPES data^{6,7}, it remains to explain why a two-gap behaviour is observed for one of the considered magnetic field directions, only. Alternatively, field-dependent spin flip has been invoked to account for this behaviour¹⁰. Besides, for few compounds, (iii) H_{c2} exhibits an upward curvature for the two field directions. More specifically, limiting ourselves to the $\text{Fe}_{1+\delta}\text{Te}_x\text{Se}_{1-x}$ chalcogenide compounds (referred to as the '11' family), all the above mentioned behaviours have been observed. Namely, behaviours (i)¹¹⁻¹⁶, (ii)^{15,17} and (iii)^{18,19} have been reported. An important question deals with the probe used for the determination of H_{c2} . As an example, while either behaviour (i) or (iii) is reported for magnetic torque data (yielding the irreversibility field), behaviour (i) is observed in specific heat data^{13,15}. Nevertheless, discrepancies are still observed using the same probe. As an example, specific heat data collected close to T_c can yield strongly different anisotropy ratios ranging from $\gamma \sim 4$ ¹³ to nearly isotropic behaviour¹¹. In that respect, crystal stoichiometry, doping and microstructure might influence the superconducting properties²⁰.

Tunnel diode oscillator (TDO) based technique, which is known to be sensitive to the London magnetic penetration depth²¹ has already been successfully used to probe H_{c2} relevant to compounds belonging to the '122' pnictide family²²⁻²⁵. Indeed, this contactless technique is very sensitive to superconducting transitions, yielding very high signal-to-noise ratio. Despite of that, to our best knowledge, no data obtained with this technique have been reported for the '11' chalcogenide superconductors, yet. Therefore, this paper reports on the determination, through TDO-based measurements, of the temperature dependence of the upper critical field of a '11' superconductor, namely $\text{FeTe}_{0.5}\text{Se}_{0.5}$, which has al-

ready been studied by magnetic torque, resistivity and specific heat^{13,15,18} measurements. The deduced physical parameters (zero-field superconducting temperature, coherence length, orbital and Pauli fields) are compared to the data obtained from these previous measurements.

II. EXPERIMENTAL

The studied $\text{Fe}_{1+\delta}\text{Te}_{0.5}\text{Se}_{0.5}$ ($\delta = 0.05$) single crystal has been synthesized using the sealed quartz tube method, as detailed in Ref. 13.

As reported in Ref. 26, the device for radio frequency measurements is a LC-tank circuit powered by a tunnel diode oscillator (TDO) biased in the negative resistance region of the current-voltage characteristic. This device is connected to a pair of compensated coils made with copper wire (40 μm in diameter). Each of these coils is wound around a Kapton tube of 1.5 mm in diameter. The studied crystal, which is a platelet with dimensions of roughly $1.4 \times 1.4 \times 0.04 \text{ mm}^3$, is placed at the centre of one of them with the normal to the conducting ab plane parallel to the coil axis. The fundamental resonant frequency f_0 of the whole set is in the range 16 to 20 MHz. This signal is amplified, mixed with a frequency f about 1 MHz below the fundamental frequency and demodulated. Resultant frequency $\Delta f = f - f_0$ has been measured in the temperature range from 1.6 K to 16 K, both in zero-field and in pulsed magnetic fields of up to 55 T with a pulse decay duration of 0.32 s. Magnetic field direction, either parallel or perpendicular to the ab plane, was explored by tilting the compensated coils so that the excitation field was always perpendicular to the ab plane. It has been checked that the data collected during the raising and the falling part of the pulse coincide, indicating that no discernible temperature change occurred during the field sweep.

III. RESULTS AND DISCUSSION

The zero-field TDO frequency displayed in Fig. 1 evidences a large increase as the temperature decreases. This feature can be ascribed to the decrease of the magnetic London penetration depth due to the superconducting transition²¹. As reported in the case of '122' pnictides²³, the onset of the frequency rise coincides with the superconducting transition deduced from *e.g.* magnetization or resistivity data. In line with this statement, the measured value ($T_c = 14.5 \text{ K}$) is in agreement with specific heat data¹³ and corresponds to the best quality samples of the considered composition²⁰.

Field-dependent TDO frequency is displayed in Figs. 2(a) and (b) for $\mathbf{H} \parallel c$ and $\mathbf{H} \parallel ab$, respectively. Well defined transitions are observed allowing to determine the temperature dependence of the upper critical magnetic field H_{c2} for the two considered field directions according to the method displayed in the in-

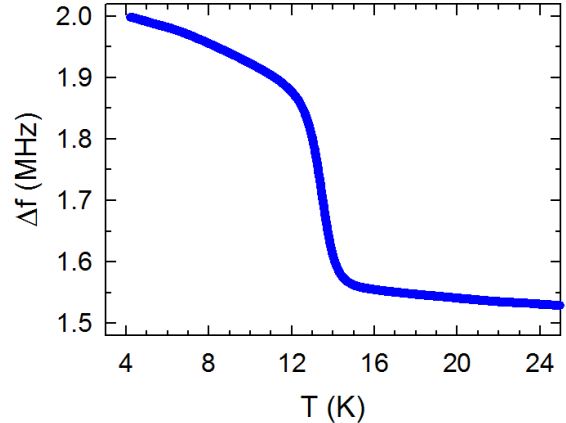


FIG. 1. (color on line) Zero-field temperature dependence of the TDO frequency.

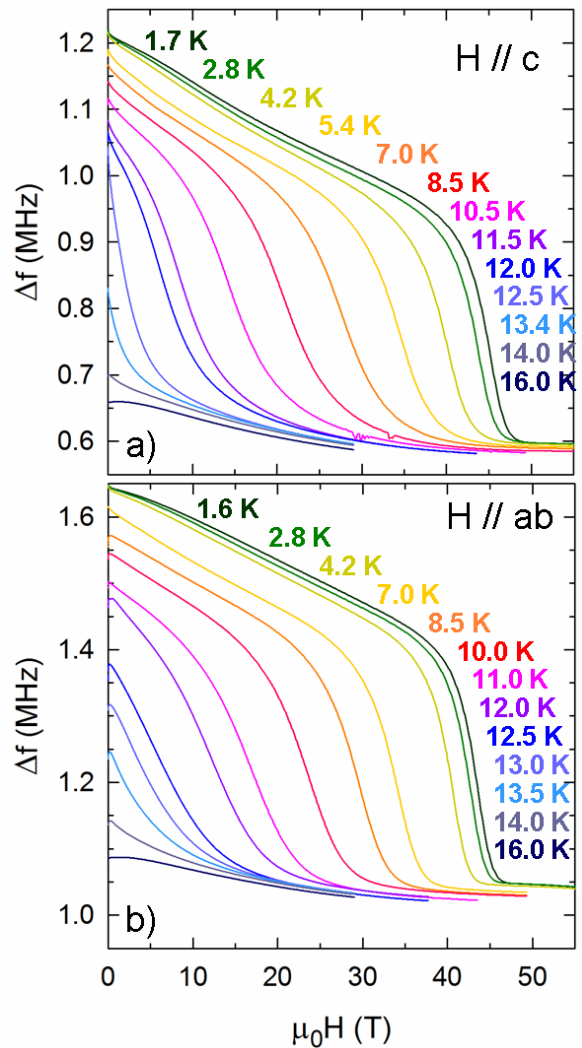


FIG. 2. (color on line) Field dependence of the TDO frequency at various temperatures for magnetic field applied parallel to (a) the c direction and (b) the ab plane.

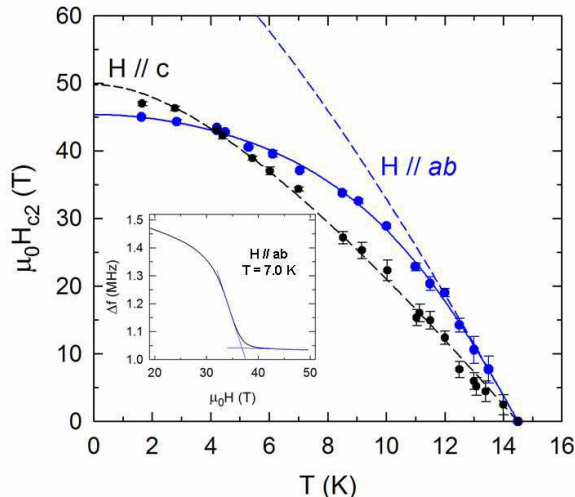


FIG. 3. (color on line) Temperature dependence of the upper critical field H_{c2} for magnetic field applied parallel to either the ab plane (blue symbols) or the c direction (black symbols). Dashed lines are the best fits of the WHH model to either the high temperature part of the data (for $\mathbf{H} \parallel ab$) or down to the lowest temperature (for $\mathbf{H} \parallel c$). Solid line is the best fit to the data for $\mathbf{H} \parallel ab$, including a Pauli contribution ($\mu_0 H_P = 79$ T). H_{c2} values are determined according to the construction lines exemplified in the insert.

sert of Fig. 3. First, in contrast with irreversibility field data¹⁸, a negative curvature is observed in both cases as reported in Fig. 3. Such a behaviour, referred above to as 'behaviour (i)', is in qualitative agreement with specific heat^{13,15} and resistivity^{11,12,14,16} measurements and indicates a single band superconductivity, in line with ARPES measurements²⁷. These data yield $dH_{c2}^{ab}/dT|_{T=T_c} = -4.9$ T/K and $dH_{c2}^c/dT|_{T=T_c} = -7.7$ T/K, hence $\gamma = 1.6$. As previously stated⁵, the slopes deduced from specific heat data are generally higher than those deduced from magnetic torque and resistivity data. Actually, the values deduced from Fig. 3, which are significantly lower than those deduced from specific heat measurements for single crystals belonging to the same batch ($dH_{c2}^{ab}/dT|_{T=T_c} = -12$ T/K and $dH_{c2}^c/dT|_{T=T_c} = -45$ T/K, respectively¹³) are in agreement with resistivity¹¹ and magnetic torque¹⁵ data. This result suggests that other contributions such as in-plane resistivity variations and vortices dynamics enter the TDO data around T_c . The above mentioned anisotropy value is rather small owing to the two-dimensional character of the Fermi surface. Nevertheless, it stays within the very scattered range reported in the literature. Indeed, limiting ourselves to specific heat data, values as different as $\gamma = 1.2^{15}$ and $\gamma = 4^{13}$ have been reported.

Dashed lines in Fig. 3 are the best fits of the WHH model²⁸ to the data, assuming negligible spin-orbit coupling³. In this framework, the temperature-dependent upper critical field is given by $\ln(1/t) =$

$\psi(1/2 + h/2t) - \psi(1/2)$ where ψ is the digamma function, $t = T/T_c$ and $h = 4\mu_0 H_{c2}/[\pi^2(-dH_{c2}/dt)|_{t=1}]$. Orbital fields deduced from the data in Fig. 3 ($\mu_0 H_{c2}^c(0) = -0.69T_c dH_{c2}/dT|_{T=T_c}$) are $\mu_0 H_{c2}^c(0) = 49$ T and $\mu_0 H_{c2}^{ab}(0) = 78$ T. These values are close to those deduced from resistivity measurements ($\mu_0 H_{c2}^c(0) = 48$ T and $\mu_0 H_{c2}^{ab}(0) = 63$ T)¹¹. However, larger values are deduced from specific heat data ($\mu_0 H_{c2}^c(0) = 130$ T and $\mu_0 H_{c2}^{ab}(0) = 400$ T¹³). Hence, the deduced coherence lengths ($\xi_c = \sqrt{(\phi_0 H_{c2}^c(0))/(2\pi)}/H_{c2}^{ab}(0) = 1.7$ nm and $\xi_{ab} = \sqrt{\phi_0/2\pi H_{c2}^c(0)} = 2.6$ nm) are closer to that derived from resistivity measurements than from specific heat data ($\xi_c = 0.4$ nm and $\xi_{ab} = 1.5$ nm)¹³.

While this model reproduces fairly well the temperature dependence of H_{c2} for $\mathbf{H} \parallel c$, Pauli pair breaking contribution must be included for $\mathbf{H} \parallel ab$. In this case, the orbital critical field is reduced as $\mu_0 H_P = \mu_0 H_{c2}^{orb}/\sqrt{1 + \alpha^2}$ where the Maki parameter is given by $\alpha = \sqrt{2H_{c2}^{orb}}/H_P$. A very good agreement with experimental data is obtained with a Pauli field $\mu_0 H_P = 79$ T, *i.e.* $\alpha = 1.4$ (see solid line in Fig. 3) yielding $\mu_0 H_{c2}(0) = 45$ T. Whereas no reliable $\mu_0 H_P$ value could be derived from specific heat data obtained at temperatures above ~ 10 K, in fields below 28 T¹³, the measured value is close to that deduced from resistivity measurements data ($\mu_0 H_P = 69$ T)¹¹. It should also be noted that the data for $\mathbf{H} \parallel c$ can be accounted for by including a small Pauli contribution ($\alpha = 0.25$), still in agreement with resistivity data. In addition, assuming strong spin-orbit coupling would yield even larger α values²⁹. Therefore, Pauli contribution for both field directions cannot be excluded.

Finally, a striking result is the anisotropy inversion occurring at 4 K ($\gamma = 0.9$ at 1.6 K). This feature, which is in line with the widely observed reduction of the anisotropy as the temperature decreases³, has already been observed at 4 K in magnetic torque¹⁵ and resistivity¹¹ measurements of $\text{FeTe}_{0.5}\text{Se}_{0.5}$. Such anisotropy inversion which had also been inferred from the extrapolation towards low temperature of specific heat data, albeit at higher temperature (~ 9 K)¹³ remains to be understood.

IV. SUMMARY AND CONCLUSION

Magnetic field- and temperature-dependent superconducting transition of single crystalline $\text{FeTe}_{0.5}\text{Se}_{0.5}$ have been studied by contactless tunnel diode oscillator-based measurements. In zero-field, the temperature dependence of the TDO frequency yields a superconducting transition temperature $T_c = 14.5$ K which is in agreement with previous specific heat, magnetic torque and resistivity data.

The WHH model accounts for the temperature dependence of the upper critical magnetic field for magnetic field applied both parallel ($\mathbf{H} \parallel ab$) and perpendicular to the conducting ab plane ($\mathbf{H} \parallel c$). This result confirms the single band nature of the superconductivity, in agreement

with ARPES data. Whereas the data can be accounted for by a negligibly small Pauli pair breaking contribution for $\mathbf{H} \parallel c$, Maki parameter $\alpha = 1.4$, corresponding to Pauli field $\mu_0 H_P = 79$ T accounts for the data for $\mathbf{H} \parallel ab$. Coherence lengths, deduced from orbital fields, and temperature sensitivity of the critical fields for the two field directions are in good agreement with resistivity data. However, orbital fields are significantly lower than those deduced from specific heat measurements. This result suggests that, in addition to magnetic London penetration depth, other contributions enter the TDO frequency variations.

Finally, the anisotropy of the critical magnetic field,

which is already rather small around T_c ($\gamma = 1.6$) becomes lower than 1 below 4 K. This result, which illustrates the commonly observed decrease of the anisotropy in iron-based superconductors as the temperature decreases, remains to be explained.

V. ACKNOWLEDGEMENTS

The authors wish to acknowledge fruitful discussions with Vitaly A. Gasparov. This work has been supported by EuroMagNET II under the EU Contract No. 228043 and by the French National Research Agency, Grant No. ANR-09-Blanc-0211 SupraTetrafer.

-
- * E-mail address: alain.audouard@lncmi.cnrs.fr
† E-mail address: loic.drigo@lncmi.cnrs.fr
‡ E-mail address: fabienne.duc@lncmi.cnrs.fr
§ Present address: Laboratoire Léon Brillouin, CEA-CNRS UMR 12, 91191 Gif-sur-Yvette Cedex, France.
- ¹ Y. Kamihara, T. Watanabe, M. Hirano and H. Hosono 2008 J. Amer. Chem. Soc. **130** 3296.
 - ² Z. Ren, L. Wei, J. Yang, Y. Wei, X.-L. Shen, Z.-C. Li, G.-C. Che X.-L. Dong, L.-L. Sun, F. Zhou, Z.-X. Zhao 2008 Chin. Phys. Lett. **25** 2215
 - ³ J.-L. Zhang, L. Jiao, Y. Chen and H. Yuan 2011 Front. Phys. **6** 463
 - ⁴ H. C. Lei, K. Wang, R. W. Hu, H. Ryu, M. Abeykoon, E. S. Bozin and C. Petrovic 2012 Sci. Technol. Adv. Mater. **13** 054305
 - ⁵ A. I. Coldea, D. Braithwaite and A. Carrington 2013 C. R. Physique **14** 94
 - ⁶ H. Ding, P. Richard, K. Nakayama, K. Sugawara, T. Arakane, Y. Sekiba, A. Takayama, S. Souma, T. Sato, T. Takahashi, Z. Wang, X. Dai, Z. Fang, G. F. Chen, J. L. Luo and N. L. Wang 2008 EPL **83** 47001
 - ⁷ L. Zhao, H. Y. Liu, W. T. Zhang, J. Q. Meng, X. W. Jia, G. D. Liu, X. L. Dong, G. F. Chen, J. L. Luo, N. L. Wang, G. L. Wang, Y. Zhou, Y. Zhu, X. Y. Wang, Z. X. Zhao, Z. Y. Xu, C. T. Chen, and X. J. Zhou, Chin. Phys. Lett., **25** 4402 (2008)
 - ⁸ Y. Zhang, Z. R. Ye, Q. Q. Ge, F. Chen, J. Jiang, M. Xu, B. P. Xie and D. L. Feng 2012 Nature Phys. **8** 371
 - ⁹ T. Yoshida, S. Ideta, T. Shimojima, W. Malaeb, K. Shinada, H. Suzuki, I. Nishi, A. Fujimori, K. Ishizaka, S. Shin, Y. Nakashima, H. Anzai, M. Arita, A. Ino, H. Namatame, M. Taniguchi, H. Kumigashira, K. Ono, S. Kasahara, T. Shibauchi, T. Terashima, Y. Matsuda, M. Nakajima, S. Uchida, Y. Tomioka, T. Ito, K. Kihou, C. H. Lee, A. Iyo, H. Eisaki, H. Ikeda, R. Arita, T. Saito, S. Onari and H. Kontani, arXiv:1301.4818.
 - ¹⁰ V. G. Kogan and R. Prozorov 2013 Phys. Rev. B **88** 024503
 - ¹¹ D. Braithwaite, G. Lapertot, W. Knafo and I. Sheikin 2010 J. Phys. Soc. Jap. **79** 053703
 - ¹² S. Khim, J. W. Kim, E. S. Choi, Y. Bang, M. Nohara, H. Takagi and K. H. Kim 2010 Phys. Rev. B **81** 184511
 - ¹³ T. Klein, D. Braithwaite, A. Demuer, W. Knafo, G. Lapertot, C. Marcenat, P. Rodière, I. Sheikin, P. Strobel, A. Sulpice and P. Toulemonde 2010 Phys. Rev. B **82** 184506
 - ¹⁴ H. C. Lei, R. W. Hu, E. S. Choi, J. B. Warren, and C. Petrovic 2010 Phys. Rev. B, **81** 94518
 - ¹⁵ A. Serafin, A. I. Coldea, A. Y. Ganin, M. J. Rosseinsky, K. Prassides, D. Vignolles, and A. Carrington 2010 Phys. Rev. B **82** 104514
 - ¹⁶ S. I. Vedenev, B. A. Piot, D. K. Maude and A. V. Sadakov 2013 Phys. Rev. B **87** 134512
 - ¹⁷ M. H. Fang, J. H. Yang, F. F. Balakirev, Y. Kohama, J. Singleton, B. Qian, Z. Q. Mao, H. D. Wang, and H. Q. Yuan 2010 Phys. Rev. B **81** 20509
 - ¹⁸ M. Bendele, S. Weyeneth, R. Puzniak, A. Maisuradze, E. Pomjakushina, K. Conder, V. Pomjakushin, H. Luetkens, S. Katrych, A. Wisniewski, R. Khasanov and H. Keller 2010 Phys. Rev. B **81** 224520
 - ¹⁹ H. C. Lei, R. W. Hu and C. Petrovic 2011 Phys. Rev. B, **84** 014520
 - ²⁰ Y. Liu and C.T. Lin 2011 J. Supercond. Nov. Magn **24** 183; V. Tsurkan, J. Deisenhofer, A. Günther, Ch. Kant, H.-A. Krug von Nidda, F. Schrettle and A. Loidl 2011 Eur. Phys. J. B **79** 289
 - ²¹ R. Prozorov and V. G. Kogan 2011 Rep. Prog. Phys. **74** 124505
 - ²² E. D. Mun, M. M. Altarawneh, C. H. Mielke, V. S. Zapf, R. Hu, S. L. Budko and P. C. Canfield 2011 Phys. Rev. B **83** 100514(R)
 - ²³ V. A. Gasparov, L. Drigo, A. Audouard, D. L. Sun, C. T. Lin, S. L. Budko, P. C. Canfield, F. Wolff-Fabris and J. Wosnitza 2011 JETP Letters **93** 667
 - ²⁴ R. Hu, E. D. Mun, M. M. Altarawneh, C. H. Mielke, V. S. Zapf, S. L. Budko and P. C. Canfield 2012 Phys. Rev. B **85** 064511
 - ²⁵ V. A. Gasparov, A. Audouard, L. Drigo, A. I. Rodigin, C. T. Lin, W. P. Liu, M. Zhang, A. F. Wang, and X. H. Chen, H. S. Jeevan, J. Maiwald, and P. Gegenwart 2013 Phys. Rev. B **87** 094508
 - ²⁶ L. Drigo, F. Durantel, A. Audouard and G. Ballon 2010 Eur. Phys. J.-Appl. Phys. **52** 10401
 - ²⁷ H. Miao, P. Richard, Y. Tanaka, K. Nakayama, T. Qian, K. Umezawa, T. Sato, Y.-M. Xu, Y. B. Shi, N. Xu, X.-P. Wang, P. Zhang, H.-B. Yang, Z.-J. Xu, J. S. Wen, G.-D. Gu, X. Dai, J.-P. Hu, T. Takahashi, and H. Ding 2012 Phys. Rev. B **85** 094506
 - ²⁸ N.R. Werthamer, K. Helfand and P.C. Hohenberg 1966 Phys. Rev. **147** 295

- ²⁹ Orlando, E. J. McNiff, Jr., S. Foner, and M. R. Beasley
1979 Phys. Rev. B **19**, 4545